WEES-2020 Special Issue

J. Indian Chem. Soc.,
Vol. 97, No. 10b, October 2020, pp. 1854-1860

Green synthesis of iron oxide magnetic nanoparticles for the adsorption of lead(II) from aqueous medium

Jamirul Islam, Parna Ganguli, Sandip Mondal* and Surabhi Chaudhuri

National Institute of Technology Durgapur, Durgapur-713 209, West Bengal, India

E-mail: san.mondal@gmail.com

Manuscript received online 01 June 2020, revised and accepted 17 October 2020

In this work, iron oxide magnetic nanoparticles (Fe_3O_4) have been synthesized using pomegranate peel extract, via green synthesis route, to remove heavy metal lead(II) from aqueous medium. Iron powder has been used as precursor agent and pomegranate peel extract has been used as reducing agent. The reaction process, i.e. co-precipitation, is simple, eco-friendly and of low cost. Synthesized adsorbent i.e. nanoparticles, were first characterized by XRD to understand the crystalline structure and phase. Also, SEM analysis was carried out to know the surface morphology of the adsorbent and the surface area of the nanoparticles were estimated using BET surface area analyzer. The average surface area of the nanoparticles was 173.38 m²/g. Average particle size was 35 nm as found in DLS analysis. The adsorption of Pb^{2+} on the surface of nano adsorbent followed pseudo-second order reaction model and Langmuir isotherm model. The maximum adsorption capacity of nano adsorbent was 142.999 mg/g. Maximum removal efficiency was observed to be 97.95% at pH 6.

Keywords: Green synthesis of nanoparticles, magnetic nanoparticles, lead removal, batch adsorption, isotherm study.

Introduction

With the increase in population, the uses of various heavy metals has increased rapidly in the field of agriculture, industries and pharmaceuticals. The main sources of heavy metals are the textile industries, dye industries, electroplating processes, metal finishing and mining operations. Heavy metals create problems when they mix with the surface water or ground water. Heavy metal contaminated waste water has potential impact on human health as well as on plants and animals. For all these reasons, removal of heavy metals is necessary from water consumed in agriculture, various industries specially food industry and domestic use. Chemical precipitation, chemical oxidation, ion exchange, ultra-filtration, electro dialysis, reverse osmosis etc. are some methods that are being used conventionally to treat heavy metal contaminated water. But all these methods are quite expensive and hence researchers are trying to search for better alternatives. Nanotechnology is an emergent discipline that is getting immense priority in various fields such as physics, chemistry, medicine, material science, environmental science etc. due to their unique properties such as small size (1–100 nm), high surface-area-to-volume ratio and tunable properties[1]. There are many established methods by which we can synthesize nanoparticles. In this project co-precipitation method has been used to synthesize the nano adsorbent (Fe_3O_4)[2]. Dave and Chopra showed that magnetic nanoparticles can be used effectively for the separation of heavy metals from aqueous solution due to inexpensive method and easy regeneration in the presence of external magnetic field[3]. Hong *et al*. used PVP-Fe_3O_4 NPs for Pb remediation from the soft water and seawater. They observed that the developed adsorbent can remove 100% of Pb within 1.5 h[4]. Lingamdinne *et al*. used tangerine peel extract for the green synthesis of iron oxide nanoparticles for lead removal from water[5]. Tamer *et al*. synthesised the iron oxide based nanoparticles by precipitation method. They observed that the removal occurred within the first 5 min of contact time and maximum uptake capacity was determined to be 166.67 mg/g[6].

In this study green synthesis of iron oxide magnetic nanoparticles has been reported as it is of low cost, environment friendly and an alternative to chemical and physical methods. Agro waste pomegranate peel is used for the

synthesis of nano adsorbent. Pomegranate peel is a rich source of large number of phenolic compounds including flavonoids and tannin. These are the main groups of antioxidants. Thereby the pomegranate peel extract is used as a reducing and capping agent in the present study[7–9]. Iron powder is used as a precursor in this synthesis.

Nanomaterials are part of the new technologies that are being used for the treatment of wastewater. In this study nano adsorbent is used for the removal of heavy metal lead (Pb(II)) from aqueous solution[1]. The main objective of this study was to synthesize iron oxide magnetic nanoparticles via green route and to assess its capability to remove lead from aqueous medium. These iron oxide nanoparticles (Fe_3O_4) has been considered to be ideal water treatment materials to remove heavy metals because of their low operating cost, magnetic properties, high adsorption capacity.

Materials and methods

Materials and chemicals:

Reagents used, namely, sodium hydroxide (NaOH), lead nitrate ($Pb(NO_3)_2$), potassium permanganate ($KMnO_4$), iron powder, 35% hydrochloric acid (HCl), ethanol were of analytical grade. Pomegranate peels were collected from local market. 0.1 *M* NaOH and 0.1 *M* HCl were used for the adjustment of pH. Whatman 42 filter paper was used for separating the adsorbent from aqueous media.

Preparation of stock solution of Pb(II):

1000 mg/L of Pb(II) stock solution was prepared by dissolving 1.614 g of $Pb(NO_3)_2$ in 1 liter of distilled water. The 50 mg/L standard Pb solution was prepared from 1000 mg/L lead solution by serial dilution method.

Synthesis of $FeCl_2$:

6 g of iron powder dissolved in 100 ml of 2 *M* HCl solutions to make 100 ml of $FeCl_2$. The chemical reaction is shown in eq. (1).

$$Fe + 2HCl = FeCl_2 + H_2 \quad (1)$$

Synthesis of $FeCl_3$:

1 *M* of $FeCl_3$ is obtained by adding 1.63 g of $KMnO_4$ in 7.5 ml of 35% 11.23 *M* HCl and 50 ml of $FeCl_2$. Color was changed from greenish to a brown after the formation of $FeCl_3$. Both the solution was filtered with Whatman filter paper. Chemical equation of the reaction has been shown in eq. (2).

$$FeCl_2 + 1/5KMnO_4 + 8/5HCl = FeCl_3 + 1/5MnCl_2 + 1/5KCl + 4/5H_2O \quad (2)$$

Preparation of pomegranate peel extract:

The pomegranate peel was collected from locally available fruit juice center located at Durgapur. The collected peel was washed with tap water followed by distilled water several times to make it dust free. After that it was dried at room temperature in dust free condition. Thereafter, the dried peel was crushed using pestle and mortar and sieved through 0.4 mm size of sieve. Obtained dry peel of 20 g powder was added to 500 ml of distilled water. It was kept for 3 h and sonicated by using probe sonicator for 10 min. After that the obtained mixture was filtered using Whatman filter 42 and centrifuged at 5000 rpm for 20 min to remove the powder particles. The obtained supernatant which acts as capping agent and reducing agent was cooled at room temperature and stored in a refrigerator at 4°C temperature for further use[7,10,11].

Synthesis of iron oxide nanoparticles (Fe_3O_4):

Iron oxide magnetic nanoparticles were synthesized by co-precipitation method. $FeCl_3$ and $FeCl_2$ were mixed in 2:1 ratio at open atmosphere. It might be possible that some portion of $FeCl_2$ got converted into $FeCl_3$. To counteract the converted portion of $FeCl_3$, $FeCl_3$ and $FeCl_2$ were mixed in 1.7:1 ratio. 1 *M* $FeCl_3$-$FeCl_2$ (1.7:1) were mixed with 100 ml of pomegranate peel extract in 1:1 ratio. Color was changed immediately from yellow to black after the addition of peel extract. Solution is then heated at 80°C temperature using heating mantle. 1 *M* freshly prepared NaOH was added drop wise to the solution under continuous stirring mode until the pH of the solution raised to pH 12. The solution mixture was stirred for 30 min to maintain the homogeneity of the solution during the reaction process[12–16].

$$Fe^{2+}(aq) + Fe^{3+}(aq) + H^+(aq) + Cl^-(aq) + NaOH(aq) = Fe_3O_4 + NaCl + H_2O \quad (3)$$

Obtained black precipitation (iron polyphenol complex) was collected by using a strong magnet or by centrifugation technique[9]. After that the particles were washed several times using distilled water and ethanol so as to remove the impuri-

ties. The precipitate was kept for drying in vacuum oven for 2–3 days at 50°C temperature for further use[17].

Characterization of adsorbent:

Synthesized adsorbent was characterized by X-ray Diffraction (XRD) with scanning range (20°–90°) to know the phase and crystalline structure. SEM analysis was carried out to know the surface morphology of the adsorbent. The surface area of the nanoparticles was estimated using BET surface area analyzer. Dynamic light scattering (DLS) test was carried out to know the particles size distribution of the adsorbent in solution.

Theory:

To find out the effect of various operating conditions on the adsorption process batch adsorption study was conducted. To optimize the maximum removal efficiency of Pb(II), the batch experiments were carried out by varying the dose, time, pH and initial concentration of the aqueous solution. The removal efficiency of Pb(II) was calculated as per the following equations[1,18]:

Removal efficiency, $R = ((C_0 - C_e)/C_0)\times 100\%$

where, C_0 = initial concentration of Pb(II) in synthetic lead solution in mg/L and

C_e = residual concentration of Pb(II) after equilibrium in mg/L.

Adsorption capacity of adsorbent was calculated as per the following equations:

q (mg/g) $= ((C_0 - C_e)\times V)/1000$ m

where, m = mass of the adsorbent in gram and

V = volume of solution in ml.

Results and discussion

BET analysis:

BET analysis was done to know the BET (Brunauer-Emmett-Teller) surface area of the developed adsorbent. BET surface area of these nanoparticles was obtained 173.3764 m^2/g i.e. significantly high. Adsorption average pore diameter (4V/A by BET) of the adsorbent was found 50.5530 Å. Average particle size was obtained 346.068 Å i.e. 34.6068 nm.

XRD characterization of Fe_3O_4 iron-oxide nanoparticles:

To determine the phase purity and crystalline nature of synthesized Fe_3O_4 iron oxide nanoparticles, X-ray diffraction (XRD) analysis of powdered nanoparticles was done. The XRD pattern of the synthesized Fe_3O_4 nanoparticles is shown in Fig. 1. XRD pattern of Fe_3O_4 nanoparticles display six relative peaks in the 2θ region of 20–70°. The main peak of the powdered nanoparticles is found at 2θ value of 35.62, which attribute to the crystalline plane with Miller indices value of 311 (JCPDF# 96-900-5813). The other peaks are observed approximately at 28.29°(202), 44.74°(400), 46.10°(333), 55.31°(404). Reflection planes of Fe_3O_4 which is matched well with the standard diffraction data of cubic inverse spinel Fe_3O_4. The peak (2θ) of the nanoparticles which was located at 2θ = 25°, 32°, 25° etc. may relate to the amorphous organic compounds adsorbed from the pomegranate peel extracts as a capping agent/stabilizing agent or due to presence of some impurities. Similar pattern was found when *Cynara carunculous* leaf extract was used as a capping agent[10,14].

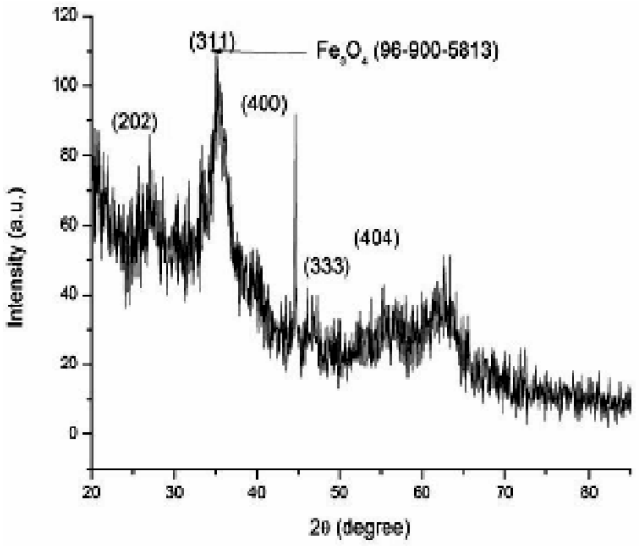

Fig. 1. XRD pattern for Fe_3O_4.

Surface morphology study of Fe_3O_4 nanoparticles:

The morphology and the size of the synthesized iron oxide nanoparticles were confirmed to be almost spherical in shape, uniform in size and nature and as in the Fig. 2, it can be seen that the particle size distribution curve of Fe_3O_4 indicated that the mean diameter size of synthesized Fe_3O_4 ION's was 31±4 nm.

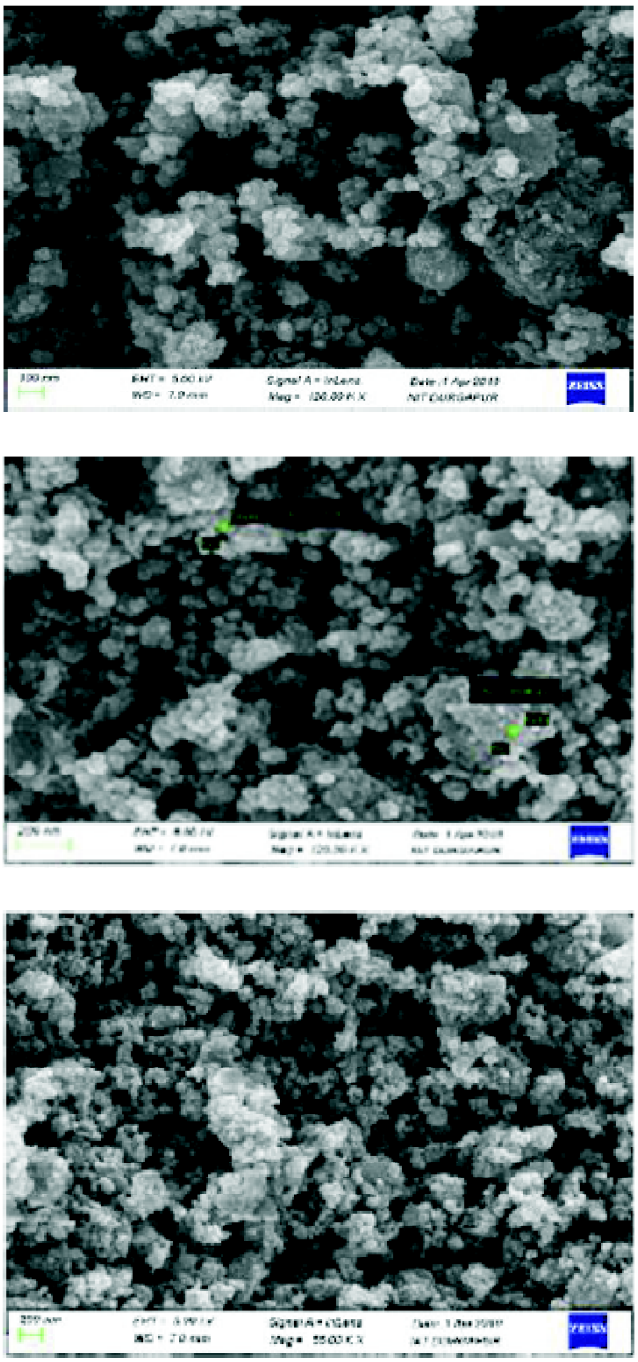

Fig. 2. FESEM image of iron oxide (Fe_3O_4) NPs at different magnification scales.

DLS analysis for size distribution:

From DLS analysis (Fig. 3) it was seen that the average particle size of adsorbent was 35 nm. This value was same as the results of SEM analysis and BET analysis.

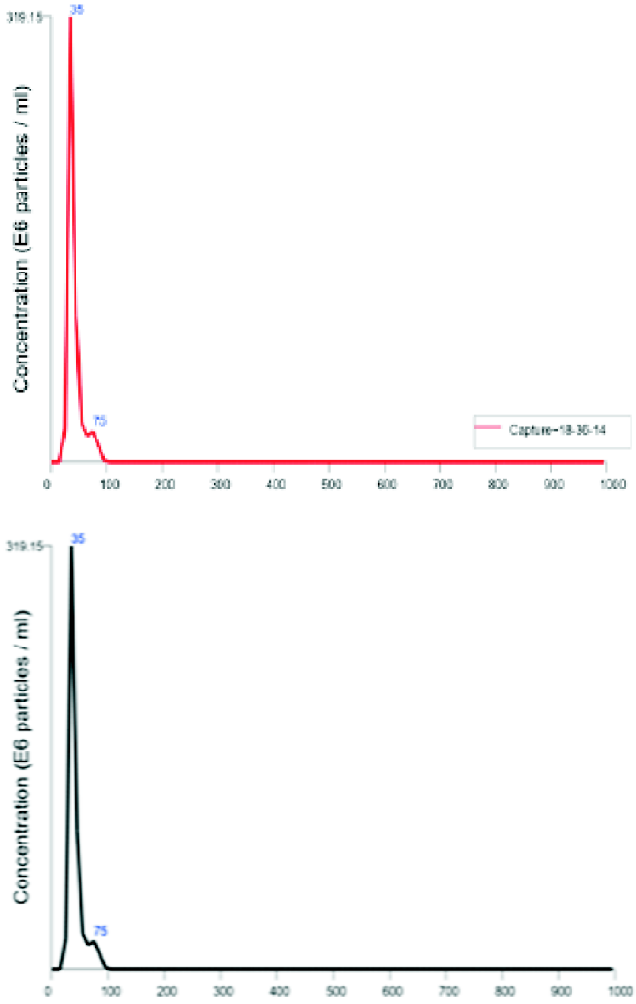

Fig. 3. DLS images of Fe_3O_4.

Zero point charge (pH_{zpc}):

Point of zero charge (pH_{zpc}) is the pH where the total charge on the surface of the adsorbent becomes zero (neutral). From Fig. 4, it can be seen that the pH_{zpc} value was obtained to be 6.4.

Batch experiments

Effect of adsorbent dose variation:

Dose variation study was conducted to observe the effects of available active sites on adsorption process. This experimental result showed that the adsorbent has very high adsorption capacity. 0.2 g/L of adsorbent dose had more than 92% removal efficiency (Fig. 5). Normally removal efficiency of lead increases with the decrease in adsorbent dose owing to the increase in surface area and active sites available for

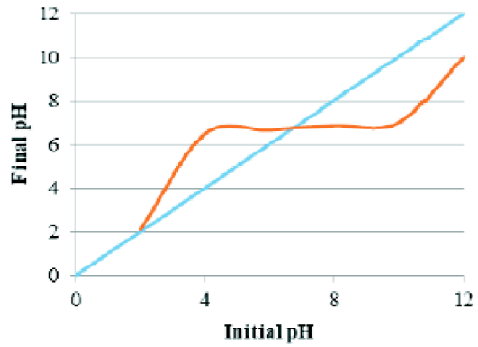

Fig. 4. Point of zero charge plot.

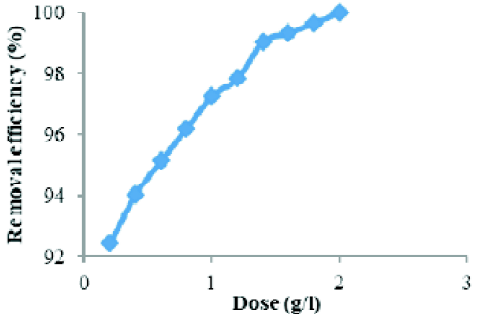

Fig. 5. Effect of dose variation on lead adsorption.

sorption[19,20]. Up to the adsorbent dose of 2.0 g/L, the removal efficiency reached more that 99%. The study concluded that in addition of little dose to the aqueous solution, a higher removal efficiency may be obtained due to the higher affinity of NPs towards the Pb(II).

Effect of initial concentration:

The effect of initial concentration study was conducted to determine the effects of adsorbate strength on the adsorption process.

The removal efficiency was very high (>99.5%) up to initial concentration of 60 mg/L at a constant adsorbent dose 1.2 g/L in the solution as shown as in Fig. 6. After that removal efficiency sharply declined and reached 91% with increasing the initial concentration of 100 mg/L. At low initial concentration, the available surface i.e. active sites of adsorbent are sufficient to adsorb most of Pb(II) ions, so the adsorption gets increased to a certain level. Further increase of initial concentration, the available sites become insufficient to adsorb Pb(II) and the removal efficiency decreases. It simply implies that the adsorbent has good enough adsorption capacity to remove lead.

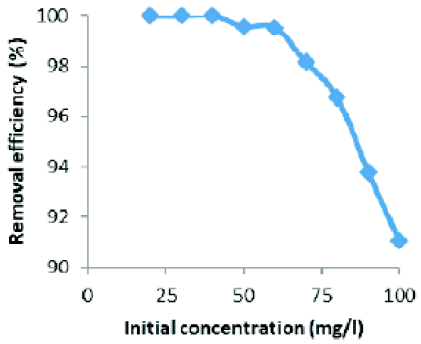

Fig. 6. Effect of initial concentration on lead adsorption.

Effect of contact time:

To determine the optimum time for the adsorption of lead ions, the experiment was conducted on Fe_3O_4 nanoparticles in aqueous solution at constant adsorbent dose of 0.2 g/L and lead concentration of 50 mg/L. It can be seen from Fig. 7 that the removal of the Pb(II) metals ions increased with the increase of the contact time as the results show that when the equilibrium reached at 50–60 min for Pb(II) metal ions, more than 87% of the lead gets removed in the first 5 min of contact time and about 90% was removed in next 20 min.

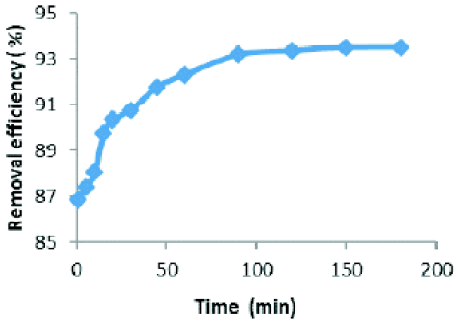

Fig. 7. Effect of contact time on lead separation.

The equilibrium is achieved very quickly due to the small size of the nanoparticles and that favor the diffusion of metal ions from the aqueous media into the active sites of the nanoparticles.

Effect of pH on Pb sorption:

The effect of pH on the adsorption process was investigated at different pH interval of the solution as the surface chemistry and metal ions solution chemistry changes significantly with change in pH. The study was conducted at constant adsorbent dose of 0.2 g/L and lead concentration of 50

mg/L. The pH value ranging from 2 to 12 for Pb(II) solution was adjusted. It is seen from Fig. 8 that the removal percentage of Pb(II) by Fe_3O_4 follows a sharp increase from 11.58% to 97.95% at pH 2 to pH 6 respectively. pH_{zpc} value of adsorbent is around 6.4 i.e. slightly acidic. At lower pH, the lead is present in the solution as free Pb^{2+} ions and high amount of strong positive charge H^+ ions surrounded to the surface of the adsorbent and that prevents Pb^{2+} ions to be removed by electrostatic repulsion[19,20]. With the increase in pH value the electrostatic repulsion starts to decline and that results in the increase in removal efficiency. At around pH = pH_{zpc} as there is no electrostatic repulsion the removal efficiency is largely increased. After that at basic conditions, electrostatic attraction force comes into picture and increases the removal efficiency. At highly basic conditions, lead ions start precipitating as hydroxide. In Fig. 8 it is seen that at pH 10, more than 98% removal efficiency is achieved. It can be concluded that the electrostatic attraction plays important role on the removal of lead from aqueous solution.

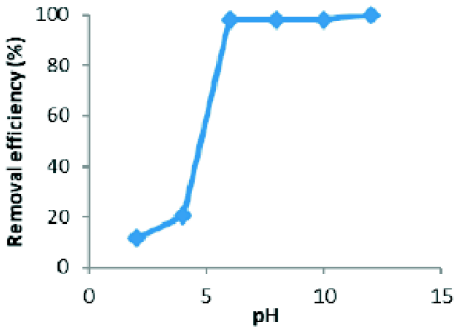

Fig. 8. Effect of pH on lead adsorption.

Kinetic model:

Equation of pseudo-first order reaction model is

$$\ln [(q_e - q_t)/q_e] = -k_{s_1} t \quad (4)$$

And equation of pseudo-second order reaction model is

$$\frac{t}{q_t} = \frac{1}{k_{s_2} q_e^2} + \frac{t}{q_t} \quad (5)$$

Kinetic data was fitted to pseudo-first order reaction model and pseudo-second order reaction model to check to absorption data of Pb^{2+}. The observed correlation coefficients (R^2) values are 1.0 and 0.996 for pseudo-second order reaction model and pseudo-first order reaction model respectively.

Isotherm model:

Different isotherm models were experienced with the isotherm data to determine the sorption mechanism. The models applied to the experimental data are given below[19,20]:

Freundlich isotherm is

$$\ln q_e = \ln K_F + (1/n) \ln C_e \quad (6)$$

Halsey equation is $K_F = \dfrac{q_m}{C_0^{1/n}}$ (7)

Langmuir isotherm equation is

$$\frac{C_e}{q_e} = \frac{1}{bq_m} + \frac{C_e}{q_m} \quad (8)$$

Experimental data were applied to Freundlich isotherm model and Langmuir isotherm model to check to absorption behavior of Pb^{2+}. The obtained results were depicted in Tables 1–3. Correlation coefficients (R^2) of Freundlich isotherm model and Langmuir isotherm model were obtained 0.932 and 0.937 respectively. K_F and n are the isotherm parameters of Freundlich isotherm to be determined. Freundlich coefficient (K_F) is 44.5673. The maximum adsorption capacity (q_m) determined from Freundlich isotherm value of Freundlich constant (n) is 3.36 i.e. greater than unity represents the adsorption of Pb^{2+} on the surface of the adsorbent is favorable adsorption. Maximum adsorption capacity (q_m) was determined from Langmuir isotherm model and obtained value is 66.67 mg/g. Langmuir constant (b) equal to 3. R_L value determined to be 0.00662 < 1 represents Pb^{2+} adsorption favor on the surface of adsorbent. Correlation coefficient (R^2) of Langmuir isotherm model is found greater than the Freundlich isotherm model.

Table 1. Parameters of pseudo-second order reaction model and pseudo-first order reaction model

Kinetic model of Pb^{2+}	K	q_e (mg/g)	R^2
Pseudo-second order reaction model	K_{s_2} = 125	250	1
Pseudo-first order reaction model	K_{s_1} = 0.03	–	0.996

Table 2. Parameters of Freundlich isotherm

Freundlich isotherm	$1/n$	K_F	q_m (mg/g)	R^2
Pb^{2+}	0.298	44.5673	142.99	0.932

Table 3. Parameters of Langmuir isotherm

Langmuir isotherm	b	R_L	q_m (mg/g)	R^2
Pb^{2+}	3	0.0062	66.67	0.937

From the batch study, it can be concluded that the adsorption of Pb^{2+} on the surface of nano adsorbent follows pseudo-second order reaction model and Langmuir isotherm model.

Conclusions

Iron oxide magnetic nanoparticles (Fe_3O_4) were synthesized via green route by co-precipitation method. Test results confirm that it is nano size having diameter around 35 nm. It is magnetic in nature having large surface area 173.3764 m^2/g. This adsorbent is suitable to remove lead(II) from aqueous solution simply by magnetic separation or by filtration. Optimum adsorption occurs at pH 6–7, contact time around 30 min, initial concentration of lead 50 mg/L and adsorbent dose 0.2 g/L. The adsorbent has attractive adsorption capacity of 66 mg/g and around 90% adsorption efficiency was achieved at optimum conditions. Due to its important physiochemical properties and low cost method these are more attractive towards water purification. Due to its high efficiency and being a low cost technology it has scope of application in various industries.

Acknowledgements

The authors are sincerely thankful to the Department of Environmental Science and Technology and the Departmental of Biotechnology of National Institute of Technology Durgapur, India.

References

1. P. L. Hariani, P. Faizal, R. M. Ridwan, M. Marsi and D. Setiabudidaya, *Int. J. Environ Sci. Te.*, 2013, **4(3)**, 336.
2. H. E. Ghandoor, H. M. Zidan, M. M. Khalil and M. I. M. Ismail, *Int. J. Electrochem. Sci*., 2012, **7(6)**, 5734.
3. P. N. Dave and L. V. Chopda, *J. Nanotech.*, 2014. **2019**, 1687.
4. J. Hong, *et al*., *RSC Adv.,* 2020, **10.6**, 3266.
5. L. P. Lingamdinne, J. R. Koduru and R. R. Karri, *Key Eng. Mater*, 2019, **805**, 3266.
6. C. Tamez, R. Hernandez and I. G. Parsons, *Microchem. J*., 2016, **125**, 97.
7. S. Venkateswarlu, S. Y. Rao, T. Balaji, B. Prathima and N. V. V. Jyothi, *Mater. Lett.*, 2013, **100**, 241.
8. H. E. Ghandoor, H. M. Zidan, M. M. Khalil and M. I. M. Ismail, *Int. J. Electrochem. Sci*., 2012, **7(6)**, 5734.
9. P. Salgado, K. Márquez, O. Rubilar, D. Contreras and G. Vidal, *Appl. Nanosci*., 2019, **9(3)**, 371.
10. S. C. Kushwaha, M. B. Bera and P. Kumar, *Chem. Asian J*., 2015, **27(12)**.
11. N. Beheshtkhoo, M. A. J. Kouhbanani, A. Savardashtaki, M. A. Amani and S. Taghizadeh, *Appl. Phys. A*, 2018, **124(5)**, 363.
12. H. Nemala, J. S. Thakur, V. M. Naik, P. P. Vaishnava, G. Lawes and R. Naik, *Int. J. Appl. Phys*., 2014, **116(3)**, 034309.
13. M. G. T. Nathan and R. Suganya, *Int. J. Pure Appl. Math*., 2018, **119(12)**, 6515.
14. S. Wu, A. Sun, F. Zhai, J. Wang, W. Xu, Q. Zhang and A. A. Volinsky, *Mater. Lett.*, 2011, **65(12)**, 1882.
15. A. Radoń, A. Drygała, L. Hawełek and D. Aukowiec, *Mater. Charact*., 2017, **131**, 148.
16. A. Radoń, A. Drygała, L. Hawełek and D. Aukowiec, *Mater. Charact*., 2017, **131**, 148.
17. A. A. Tayel, A. F. El-Baz, M. F. Salem and M. H. El-Hadary, *J. Plant Dis. Prot*., 2009, **116(6)**, 252.
18. P. L. Hariani, M. Faizal, R. Ridwan, M. Marsi and D. Setiabudidaya, *Int. J. Environ. Sci. Te*., 2013, **4(3)**, 336.
19. S. Mondal and C. Mahanta, *Desalin. Water Treat*., 2017, **84**, 309.
20. R. Kumar and S. Mondal, "Removal of Fluoride from Aqueous Solution Using Coal-Coated with $FeCl_3$", in: Recent Developments in Waste Management, Springer, Singapore, 2020, 417.